

ORIGINAL ARTICLE

18F-FDG-PET/CT versus 99Tcm-MIBI-SPECT: which is better for detection of solitary pulmonary nodules ?

Guoliang Xia¹, Chuanguo An², Zonghua Ming³, Hong Guo³, Lihong Liu⁴, Yufeng Li⁵

¹Department of Nuclear Medicine, People`s Hospital of Rizhao, China; ²Department of General Surgery, People`s Hospital of Rizhao, China; ³Health Management Center, People`s Hospital of Zhangqiu, China; ⁴ECG room, People`s Hospital of Zhangqiu, China; ⁵Department of Oncology, People`s Hospital of Rizhao, China

Summary

Purpose: To compare the diagnostic value of 99Tcm-MIBI-SPECT and 18F-FDG-PET/CT in differentiating benign from malignant solitary pulmonary nodules (SPNs).

Methods: 170 SPNs were involved in this study (78 with 99Tcm-MIBI-SPECT and 92 with 18F-FDG-PET/CT). Definite diagnosis of SPNs was determined by biopsy. The diagnostic efficiency of 99Tcm-MIBI-SPECT and 18F-FDG-PET/CT in differentiating benign from malignant SPNs was analyzed and compared.

Results: Seventy-eight patients with SPNs were examined with 99Tcm-MIBI-SPECT (26 with malignant SPNs and 52 with benign SPNs). The sensitivity, specificity and accuracy of 99Tcm-MIBI-SPECT were 92.31, 88.46 and 89.74%, respectively. The positive predictive value (PPV) and negative predictive value (NPV) were 80 and 95.83%, respectively. Ninety-two individuals with SPNs were examined using

18F-FDG-PET/CT (58 with malignant SPNs and 34 with benign SPNs). The sensitivity, specificity and accuracy of 18F-FDG-PET/CT were 96.55, 76.47 and 89.13%, respectively. The PPV and NPV were 87.50 and 92.86%, respectively. Statistical significance was not detected in sensitivity, specificity, accuracy, PPV and NPV between these two methods.

Conclusion: 99Tcm-MIBI-SPECT has comparable diagnostic value with 18F-FDG-PET/CT in differentiating benign from malignant SPNs. Considering its easy availability and low-cost, 99Tcm-MIBI-SPECT could be an alternative imaging modality in differentiating benign from malignant SPNs in areas with a backward economy.

Key words: 99Tcm-MIBI, SPECT, 18F-FDG, PET/CT, solitary pulmonary nodules, lung cancer

Introduction

SPN is a common morphologic feature in the early stage of lung cancer [1]. About 1/3 SPNs could be differentiated by typical radiologic methods and 2/3 need to be further determined by invasive methods [2,3]. It is of great clinical value to differentiate benign from malignant SPNs accurately and timely. On one hand there will be no delay in the operation of patients with malignant tumors and on the other hand thoracic operations-related complications in patients with benign tumors could be avoided. Non-invasive diagnostic techniques currently used for evaluating SPN in-

clude sputum cytology, chest radiography, computed tomography (CT) and positron emission tomography (PET). F-18 fluorodeoxyglucose (FDG) PET (18F-FDG PET) is becoming widely used for differentiating benign from malignant nodules [4,5]. PET performed with 18F-FDG is recognized as an imaging modality with a unique capability of differentiating malignant from normal tissue on the basis of the Warburg effect. 18F-FDG-PET/CT uses 18F-FDG as a marker of metabolism within lesions. The concentration of 18F-FDG localized in lesions is proportionate to their metabolic activity.

Correspondence to: Yufeng Li, Mast Med. Department of Oncology, People`s Hospital of Rizhao. 126 Taian Road, 276800 Rizhao, Shandong, China.

Tel: +86 015610509062, E-mail: chenzfrz@163.com

Received: 16/06/2017; Accepted: 27/06/2017

SPNs with higher activity of metabolism than the mediastinal blood pool are likely malignant SPNs.

In recent years, Tc-99m methoxyisobutylisonitrile (MIBI) SPECT (99Tcm-MIBI SPECT) is widely applied as a kind of myocardial perfusion-imaging [6]. Given that it can be accumulated in tumors, 99m Tcm-MIBI was widely used in tumor research and is well known to be useful in detecting primary tumors and metastases [7]. 99Tcm-MIBI SPECT has good imaging quality, and is also suitable for single photon emission computed tomography imaging (SPECT).

We conducted this current study to compare the diagnostic efficiency of 99Tcm-MIBI SPECT and 18F-FDG-PET/CT for SPNs.

Methods

Imaging criteria for SPN

Patients with SPNs which were detected by CT were selected. SPNs were defined as single, round or oval opaque lesions which were surrounded completely by lung parenchyma and less than 3 cm in diameter with no enlarged lymph nodes, atelectasis or pneumonia [8]. SPNs characterized by benign radiologic features (central, diffuse or popcorn-like calcification) or malignant radiologic features (radiate corona, spotted or eccentric calcification) were excluded from the study [9].

99Tcm-MIBI SPECT group

In this study enrolled were 78 patients (45 male and 33 female) showing SPNs on CT and having done 99Tcm-MIBI SPECT between February, 2014 and August, 2016. The age of patients ranged from 37 to 77 years (mean±SD 55.34±10.09). The diameters of SPNs ranged from 0.57 to 2.89 cm (mean ± SD 1.77±0.75). Thirty-five, 10 and 33 SPNs were located in the upper, middle and lower lobe, respectively.

18F-FDG-PET/CT group

Ninety-two patients (54 male and 38 female) showing SPNs on CT and having done 18F-FDG-PET/CT between January, 2014 and September, 2016 were enrolled in this study. The age of patients ranged from 35 to 81 years (mean±SD 56.72±12.03). The diameters of SPNs ranged from 0.61 to 3.03 cm (mean±SD 2.13±0.67). Of the SPNs 41, 6 and 45 were located in the upper, middle and lower lobe, respectively.

All of the patients in the two groups were definitely diagnosed with postoperative biopsy. There was

no statistical significance in gender ($\chi^2=2.189$, $p=0.153$), age ($t=0.067$, $p=0.971$), locations of SPNs in the lung ($\chi^2=1.432$, $p=0.605$) and diameters of SPNs ($t=1.731$, $p=0.138$) between the two groups (Table1).

99Tcm-MIBI SPECT

99Tcm and MIBI were provided by Beijing Atom Hitech Co. Ltd and Beijing Shihong Drug Development Center, respectively. The radiochemical purity of 99Tcm-MIBI was >95%. The SPECT-CT equipment was purchased from Infinia Vc HawKeye, (GE Healthcare, Little Chalfont, Buckinghamshire, UK). Before 99Tcm-MIBI injection, the subjects were administered oxygen inhalation through nasal catheter with initial oxygen flow of 5 L/min that gradually increased to 10 L/min (2 cases with high flow oxygen showed obvious discomfort and their maximum flow was 7 L/min). Patients received 740 MBq 99Tcm-MIBI by intravenous injection in the arm contralateral to the thoracic mass after they consistently inhaled oxygen with 10 L/min for 8 min. Then they continued to inhale oxygen for 2 min [10]. Ten-min (early image) and 120-min (delayed image) post-injection, SPECT constructed fusion imaging equipped with a low energy and high resolution parallel hole collimator. The energy peak was centered at 140 Kev with a 20% window, using a 128×128 matrix, at 30 s per view. Images were collected for 360° with magnification of 1.0 time. The whole lung images were obtained with scanning current of 2.5 mA, voltage of 140 kV at a rotational speed of 2.6 r/min. Attenuation correction and reconstruction of SPECT were automatically processed by ordered-subsets expectation maximization (OSEM) coming with the instrument. Volumetric for HawKeye was used to fuse images from SPECT and CT where the slice thickness of SPECT was 4.42 mm. Qualitative imaging diagnostic criteria included: (1) lesions detected by CT should have higher radioactivity than peripheral and contralateral pulmonary tissue; (2) Maximal intensity projection (MIP) should show the radioactive concentration of focal lesions that were consistent with the location of the lung lesions. Images with both (1) and (2) were determined as positive while they were considered as negative when the radioactivity of lung lesions was similar to that of peripheral and contralateral lung tissue. Manual regions of interest (ROI) were drawn over the tumor area with the highest radioactivity and another ROI of the same size over the symmetrical normal lung area on the contralateral side in transverse slices. Then, the mean early uptake ratios (EUR) and delayed uptake ratios (DUR) were calculated semi-quantitatively. The data for EUR and DUR were expressed as mean ±standard deviation and 95% confidence interval (95% CI).

Table 1. Demographic data of the patients in the two groups

	Gender			Age (y)		Diameter (cm)		Location of the single nodules		
	Male	Female	Total	Range	Mean ± SD	Range	Mean ± SD	Upper lobe	Middle lobe	Lower lobe
99Tcm-MIBI SPECT	45	33	78	37-77	55.34 ± 10.09	0.57-2.89	1.77 ± 0.75	35	10	33
18F-FDG-PET/CT	54	38	92	35-81	56.72 ± 12.03	0.61-3.03	2.13 ± 0.67	41	6	45

18F-FDG-PET/CT

Patients were injected with ^{18}F -FDG (5.55 MBq/kg) intravenously after fasting more than 6 hrs and a rest for 15-20 min. Then, they rested on bed away from light. PET/CT scanning (Siemens Biograph 16, Berlin, Germany) was performed 50-60 min after injection. The images obtained ranged from vertex to mid-thigh. 3D mode was utilized to collect images with 6-7 beds and 1.5 min/bed. The voltage and current were 120 kV and 200 mA, respectively. Raw CT data was reconstructed using B20f smooth with 1.5 mm slice thickness and 3.0 mm increment. CT data was used for attenuation correction of PET images and OSEM for PET images reconstruction. ^{18}F -FDG with radiochemical purity of >95% was produced by cyclotron (HM10 Sumitomo Corporation, Tokyo, Japan) and automatic chemical synthesis module in our center. Combining images of CT and PET, we diagnosed qualitatively through the uptake degree of ^{18}F -FDG, locations and morphology of lesions. Manual ROI were drawn over the tumor area with highest radioactivity which included all pixels with radioactivity >90%. To decrease the influence of ROI on standardized uptake value (SUV), the maximum SUV (SUVmax) was used as standard in which SUVmax ≥ 2.5 was defined as positive and <2.5 as negative [11].

Statistics

Sensitivity, specificity, accuracy, PPV and NPV were used in the qualitative analysis. Statistical analyses were performed using SPSS Version 18.0 (Chicago: SPSS Inc). Chi-square test was used for qualitative data. Two independent sample *t*-test was used for EUR, DUR and SUVmax. The diagnostic efficiency of EUR, DUR and SUVmax were analyzed using receiver operating characteristic (ROC) method. P value <0.05 was considered statistically significant.

Results*99Tcm-MIBI SPECT*

Among the 78 SPNs, 26 cases (13 lung adenocarcinoma, 7 lung squamous cell carcinoma, 2 lung small cell carcinoma, 2 metastasis of laryngeal cancer and 2 breast malignant fibrous histiocytoma) were confirmed as malignant tumors by biopsy. Fifty-two cases (15 tuberculosis, 13 lung inflammation, 4 fibroplasia, 2 hamartoma and 1 chronic purulent inflammation and 17 cases of undefined SPNs whose diameters did not change

Table 4. Comparison of diagnostic efficiency between ^{99}Tcm -MIBI SPECT and ^{18}F -FDG-PET/CT in single pulmonary nodules

	<i>Sensitivity</i>	<i>Specificity</i>	<i>Accuracy</i>	<i>PPV</i>	<i>NPV</i>
^{99}Tcm -MIBI SPECT	24/26	46/52	70/78	24/30	46/48
^{18}F -FDG-PET/CT	28/29	26/34	82/92	56/64	26/28
χ^2	0.356	1.084	0.008	0.453	0.157
<i>p</i>	0.55	0.298	0.927	0.501	0.692

PPV: positive predictive value, NPV: negative predictive value

for more than 2 years) were diagnosed as benign lesions by biopsy. Thirty positive (24 true positive and 6 false positive) and 48 negative (46 true negative and 2 false negative) cases were defined by ^{99}Tcm -MIBI SPECT (Table 2).

Table 2. Diagnostic results of ^{99}Tcm -MIBI-SPECT in single pulmonary nodules

		<i>Biopsy</i>		<i>Total</i>
		+	-	
^{99}Tcm -MIBI SPECT	+	24	6	30
	-	2	46	48
Total		26	52	78

18F-FDG-PET/CT

Among the 92 SPNs, 58 cases (41 lung adenocarcinoma, 13 lung squamous cell carcinoma, 2 lung small cell carcinoma, 2 lung adenosquamous carcinoma) were confirmed as malignant tumors by biopsy. Thirty-four cases (5 tuberculosis, 6 inflammatory pseudotumor, 8 inflammatory granuloma, 2 chronic purulent inflammation and 13 undefined SPNs whose diameters did not change for more than 2 years) were diagnosed with benign lesions. Sixty positive (56 true positive and 8 false positive) and 28 negative (26 true negative and 2 false negative) cases were defined by ^{18}F -FDG-PET/CT (Table 3).

Table 3. Diagnostic results of ^{18}F -FDG-PET/CT in single pulmonary nodules

		<i>Biopsy</i>		<i>Total</i>
		+	-	
^{99}Tcm -MIBI SPECT	+	56	8	64
	-	2	26	28
Total		58	34	92

Comparison of diagnostic efficiency between ^{99}Tcm -MIBI SPECT and ^{18}F -FDG-PET/CT in SPNs

According to Table 2, the sensitivity, specificity and accuracy of ^{99}Tcm -MIBI SPECT were 92.31 (24/26), 88.46 (46/52) and 89.74% (70/78), respectively. PPV and NPV were 80 (24/30) and 95.83% (46/48), respectively.

According to Table 3, the sensitivity, specificity and accuracy of 18F-FDG-PET/CT were 96.55 (28/29), 76.47 (26/34) and 89.13% (82/92), respectively. The PPV and NPV were 87.50 (56/64) and 92.86% (26/28, respectively). Statistical difference was not detected in sensitivity, specificity, accuracy, PPV and NPV between these two methods (Table 4).

Discussion

Because of the increase of transmembrane potential difference of tumor cells and potential gradient of the inner and outer membrane of the mitochondria caused by gene mutation, the concentration of ⁹⁹Tcm-MIBI in malignant tumor cells is about 10-fold higher than that in normal cells [12]. In addition, active tumor cells' ⁹⁹Tcm-MIBI uptake is more owing to fast growth, higher metabolism level and abnormal membrane potential [12]. Mitochondria are the major site of energy metabolism. Just as the aggregation of 18F-FDG in cells reflects glucose metabolism, the degree of aggregation of ⁹⁹Tcm-MIBI in cells may partly reflect the energy metabolism of the cells [13]. The current study indicated that ⁹⁹Tcm-MIBI can be used as a tracer to differentiate benign from malignant SPNs. A study has shown that the sensitivity, specificity, accuracy, PPV and NPV of ⁹⁹Tcm-MIBI SPECT/CT in diagnosing SPNs were all more than 90% [14]. On the basis of reported studies [13,15,16], we analyzed the diagnostic value of ⁹⁹Tcm-MIBI SPECT in differentiating SPNs. Also, this is the first study to compare the diagnostic efficiency of ⁹⁹Tcm-MIBI SPECT and 18F-FDG-PET/CT in differentiating benign from malignant SPNs.

In this study, the diagnostic efficiency of ⁹⁹Tcm-MIBI SPECT was similar to that of 18F-FDG-PET/CT and was in accordance with the Sergiacomi et al. [17] and Kim et al. reports [18], respectively. Santini et al. [19] reported that both

⁹⁹Tcm-MIBI SPECT and 18F-FDG-PET had similar diagnostic value for undefined SPNs. The current study focused on SPNs which were confined to lung tissue. The early detection and differentiation of SPNs is valuable for patients with malignant tumors because they could be subjected to operation early. Although SPNs enrolled in our study did not show any typical benign or malignant CT imaging features, CT images can not only locate lesions in the lung exactly to avoid misjudging radioactivity accumulation in normal tissue as lesions but also to correct attenuation of SPECT or PET [19]. What's more, the sensitivity of ⁹⁹Tcm-MIBI SPECT and 18F-FDG-PET/CT in our study in diagnosing SPNs was higher than that in another report [19] (92.31 vs 83.30%, and 96.55 vs 88.80%). The high NPV of ⁹⁹Tcm-MIBI SPECT and 18F-FDG-PET/CT was consistent with the reports of other authors [17,18]. In the two groups 2 FN cases (both were lung adenocarcinomas) were detected, respectively. Most negative patients can be excluded by ⁹⁹Tcm-MIBI SPECT or 18F-FDG-PET/CT, thereby avoiding thoracic operations. With different uptake mechanisms of MIBI and FDG by tumor cells, the combination and complementation of these two tracers may provide more biological information of tumors [20].

We were not able to notice any statistical difference in sensitivity and specificity between these two methods in diagnosing SPNs. In the ⁹⁹Tcm-MIBI SPECT group, pulmonary hilar radioactive concentration was found in 6 cases with malignant tumors which were confirmed as metastatic lymph node lesions by pathology (Figure 1). In the 18F-FDG-PET/CT group, pulmonary hilar and/or mediastinum radioactive concentration were found in 27 cases which were confirmed as metastatic lymph node lesions by pathology (Figure 2). In addition, ⁹⁹Tcm-MIBI SPECT and 18F-FDG-PET/CT can not only be used in differentiating benign from malignant SPNs, but also in evaluating and predicting chemotherapeutic

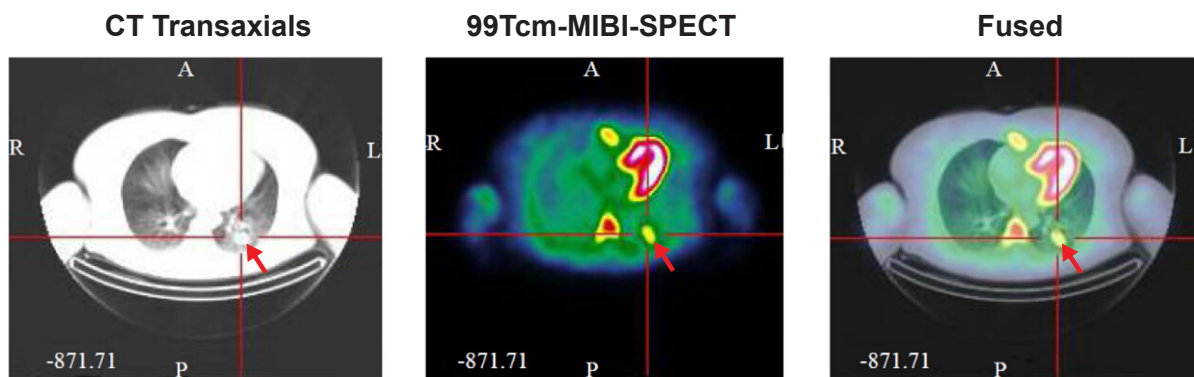


Figure 1. Imaging findings using ⁹⁹Tcm-MIBI SPECT of a 49-year-old female patient with malignancy. The lesion was pathologically diagnosed as metastatic lymph node.

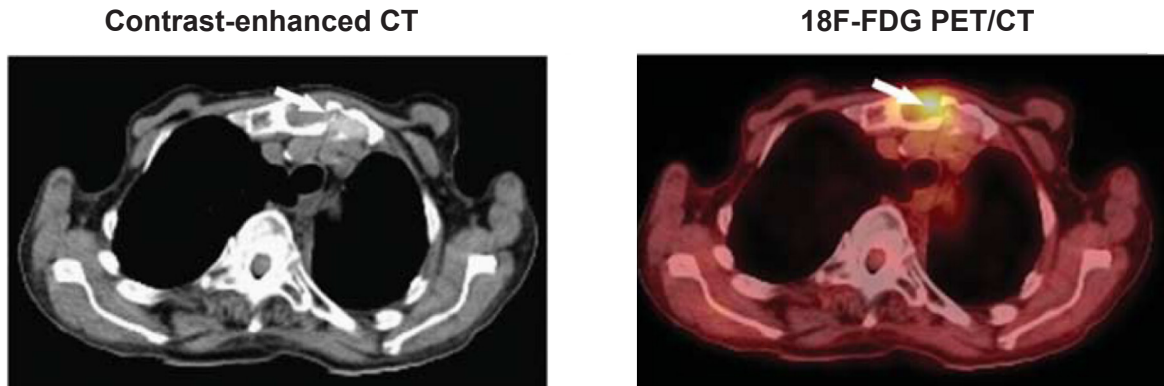


Figure 2. Accumulation in contrast-enhanced 18F-FDG/CT in a 79-year-old patient with bone metastasis from NSCLC (arrow: metastasis focus), pathologically confirmed as metastatic lymph node.

response. Cecchin et al. [21] reported that ^{99}Tcm -MIBI has been used in evaluating multi-drug resistance (MDR) and predicting chemotherapeutic response. Ambrosini et al. [22] indicated that several times examination of PET were significant to evaluating chemotherapeutic response of post chemotherapeutic patients with small cell lung cancer.

Some limitations in the current study should be acknowledged. Firstly, the number of patients enrolled in our study was rather small. Secondly, the data of whether pulmonary hilar and/or mediastinal lymph nodes were invaded was incomplete, which is very important to staging malignant SPNs. As a result, we could not come to any definite conclusions. The diagnostic value of ^{99}Tcm -MIBI SPECT in recognizing metastatic

pulmonary hilar and/or mediastinal lymph nodes will be the focus in future studies.

In conclusion, ^{99}Tcm -MIBI SPECT had comparable diagnostic value with 18F-FDG-PET/CT in differentiating benign and malignant SPNs in our study. ^{99}Tcm -MIBI SPECT is a kind of inexpensive, noninvasive modality and also a valuable diagnostic method for SPNs. Considering its easy availability and low-cost, ^{99}Tcm -MIBI SPECT could be an alternative imaging modality in differentiating benign from malignant SPNs in areas with a backward economy where 18F-FDG-PET/CT is not available.

Conflict of interests

The authors declare no conflict of interests.

References

- Jing X, Lin Y, Zhang B, Zhang G. Video-assisted thoracoscopic lobectomy mitigates adverse oncological effects of delayed adjuvant chemotherapy for non-small cell lung cancer patients. *J BUON* 2016;21:1524-9.
- Yaffe D, Koslow M, Haskiya H, Shitrit D. A novel technique for CT-guided transthoracic biopsy of lung lesions: Improved biopsy accuracy and safety. *Eur Radiol* 2015;25:3354-60.
- Conti V, Petroianni A, Halili I et al. A woman with a solitary pulmonary nodule: Is it a lung cancer? *Eur Rev Med Pharmacol Sci* 2012;16 (Suppl 4):38-41.
- Cook GJ, O'Brien ME, Siddique M et al. Non-small cell lung cancer treated with erlotinib: Heterogeneity of (18)F-FDG uptake at PET-Association with treatment response and prognosis. *Radiology* 2015;276:883-93.
- Taus A, Aguilo R, Curull V et al. Impact of 18F-FDG PET/CT in the treatment of patients with non-small cell lung cancer. *Arch Bronchopneumol* 2014;50:99-104.
- Klein R, Hung GU, Wu TC et al. Feasibility and operator variability of myocardial blood flow and reserve measurements with (9)(9)mTc-sestamibi quantitative dynamic SPECT/CT imaging. *J Nucl Cardiol* 2014;21:1075-88.
- Nikoletic K, Mihailovic J, Srbovan D et al. Lung tumors: Early and delayed ratio of ^{99}mTc -methoxy-2-isobutylisonitrile accumulation. *Vojnosanit Pregl* 2014;71:438-45.
- Wahidi MM, Govert JA, Goudar RK et al. Evidence for the treatment of patients with pulmonary nodules: When is it lung cancer?: ACCP evidence-based clinical practice guidelines (2nd Edn). *Chest* 2007;132: 94S-107S.
- Ambrosini V, Rubello D. Is there an ideal diagnostic algorithm in solitary pulmonary nodules? *Respiration* 2006;73:587-9.
- Cermik TF, Altıay G, Firat MF et al. Assessment of Tc-99m sestamibi tumor tissue uptake under the influence of increased arterial oxygen saturation. *Nucl*

- Med Biol 2005;32:165-70.
11. Macdonald K, Searle J, Lyburn I. The role of dual time point FDG PET imaging in the evaluation of solitary pulmonary nodules with an initial standard uptake value less than 2.5. *Clin Radiol* 2011;66:244-50.
 12. Moretti JL, Hauet N, Caglar M et al. To use MIBI or not to use MIBI? That is the question when assessing tumour cells. *Eur J Nucl Med Mol Imaging* 2005;32:836-42.
 13. Nikoletic K, Lucic S, Peter A et al. Lung 99mTc-MIBI scintigraphy: Impact on diagnosis of solitary pulmonary nodule. *Bosn J Basic Med Sci* 2011;11:174-9.
 14. Furuta M, Nozaki M, Kawashima M et al. Monitoring mitochondrial metabolisms in irradiated human cancer cells with (99m)Tc-MIBI. *Cancer Lett* 2004;212:105-11.
 15. Santini M, Fiorello A, Mansi L et al. The role of technetium-99m hexakis-2-methoxyisobutyl isonitrile in the detection of neoplastic lung lesions. *Eur J Cardiothorac Surg* 2009;35:325-31.
 16. Schuurmans MM, Ellmann A, Bouma H et al. Solitary pulmonary nodule evaluation with 99mTc-methoxyisobutyl isonitrile in a tuberculosis-endemic area. *Eur Respir J* 2007;30:1090-5.
 17. Sergiacomi G, Schillaci O, Leporace M et al. Integrated multislice CT and Tc-99m Sestamibi SPECT-CT evaluation of solitary pulmonary nodules. *Radiol Med* 2006;111:213-24.
 18. Kim SK, Allen-Auerbach M, Goldin J et al. Accuracy of PET/CT in characterization of solitary pulmonary lesions. *J Nucl Med* 2007;48:214-20.
 19. Santini M, Fiorelli A, Vicidomini G et al. F-18-2-fluoro-2-deoxyglucose positron emission tomography compared to technetium-99m hexakis-2-methoxyisobutyl isonitrile single photon emission chest tomography in the diagnosis of indeterminate lung lesions. *Respiration* 2010;80:524-33.
 20. Higashi K, Ueda Y, Matsunari I et al. 11C-acetate PET imaging of lung cancer: Comparison with 18F-FDG PET and 99mTc-MIBI SPET. *Eur J Nucl Med Mol Imaging* 2004;31:13-21.
 21. Cecchin D, Schiorlin I, Della PA et al. Assessing response using 99mTc-MIBI early after interstitial chemotherapy with carmustine-loaded polymers in glioblastoma multiforme: Preliminary results. *Biomed Res Int* 2014;2014:684383.
 22. Ambrosini V, Nicolini S, Caroli P et al. PET/CT imaging in different types of lung cancer: An overview. *Eur J Radiol* 2012;81:988-1001.